

Communication

# Coherence transfer between spy nuclei and nitrogen-14 in solids

Simone Cavadini<sup>a,\*</sup>, Anuji Abraham<sup>a</sup>, Geoffrey Bodenhausen<sup>a,b,c</sup>

<sup>a</sup> *Laboratoire de Résonance Magnétique Biomoléculaire, Institut des Sciences et Ingénierie Chimiques, Ecole Polytechnique Fédérale de Lausanne, Batochime, CH-1015 Lausanne, Switzerland*

<sup>b</sup> *Département de Chimie, associé au CNRS, Ecole Normale Supérieure, 24 rue Lhomond 75231, Paris Cedex 05, France*

<sup>c</sup> *Department of Chemistry, University of California at Berkeley, CA, USA*

Received 29 June 2007; revised 12 October 2007

Available online 18 October 2007

## Abstract

Coherence transfer from ‘spy nuclei’ such as  $^1\text{H}$  or  $^{13}\text{C}$  ( $S = 1/2$ ) was used to excite single- or double-quantum coherences of  $^{14}\text{N}$  nuclei ( $I = 1$ ) while the  $S$  spins were aligned along the static field, in the manner of heteronuclear single-quantum correlation (HSQC) spectroscopy. For samples spinning at the magic angle, coherence transfer can be achieved through a combination of scalar couplings  $J(I, S)$  and second-order quadrupole–dipole cross-terms, also known as residual dipolar splittings (RDS). The second-order quadrupolar powder patterns in the two-dimensional spectra allow one to determine the quadrupolar parameters of  $^{14}\text{N}$  in amino acids.

© 2007 Elsevier Inc. All rights reserved.

**Keywords:** Solid-state NMR; Magic angle spinning (MAS); Nitrogen-14 NMR; Quadrupolar parameters; HSQC; HMQC; Amino acids

Efficient detection of  $^{14}\text{N}$  nuclei (99.6% natural abundance) is of interest since nitrogen is involved in the architecture of many materials, including biomolecules such as proteins and nucleic acids. Information about the quadrupolar coupling constant  $C_Q$  and asymmetry parameter  $\eta_Q$ , which may help to determine the molecular structure and characterize local dynamics, can be extracted from the second-order quadrupolar  $^{14}\text{N}$  powder patterns in single- and double-quantum spectra in samples spinning at the magic angle. Because of the large quadrupole coupling constants [1–4],  $^{14}\text{N}$  NMR was regarded as a difficult challenge until recently, but the advent of indirect detection via spy nuclei with  $S = 1/2$  such as  $^{13}\text{C}$  or  $^1\text{H}$  made  $^{14}\text{N}$  NMR in solids relatively straightforward. The indirect observation of  $^{14}\text{N}$  single-quantum (SQ) or double-quantum (DQ) spectra is possible by transferring coherence to and fro between spins  $S$  and  $I$  via a combination of scalar couplings and second-order quadrupole–dipole cross-terms, also known as residual dipolar splittings (RDS), [5–10] or by recoupling the heteronuclear dipolar interactions by suitable se-

quences of radio-frequency (RF) pulses [11–16]. The methods proposed so far were built on the model of what has come to be known in liquid-state NMR as ‘heteronuclear multiple-quantum correlation’ (HMQC) [17–19], where heteronuclear two-spin coherences such as  $S_x I_x$  or  $S_x I_x^2$  evolve in the  $t_1$  intervals of the two-dimensional experiments. In the present study, we have adapted the scheme known in liquids as ‘heteronuclear single-quantum correlation’ (HSQC) [20,21], where homonuclear  $^{14}\text{N}$  single-quantum (SQ) and double-quantum (DQ) coherences such as  $S_z I_x$  or  $S_z I_x^2$  that are antiphase with respect to the spy nucleus  $S$  precess in the  $t_1$  evolution period.

Fig. 1 shows an HSQC sequence for the indirect detection of  $^{14}\text{N}$  SQ or DQ spectra in solids rotating at the magic angle. These experiments exploit a combination of scalar couplings  $J(I, S)$  and second-order quadrupole–dipole cross-terms or residual dipolar splittings between  $^1\text{H}$  or  $^{13}\text{C}$  ( $S$ ) and  $^{14}\text{N}$  ( $I$ ) nuclei for the transfer of coherence from spin  $S$  to  $I$  and back. If  $^{13}\text{C}$  nuclei are used as spies cross polarization (CP) from  $^1\text{H}$  to  $^{13}\text{C}$  can be used for the initial enhancement of  $^{13}\text{C}$  coherence, and heteronuclear  $^1\text{H}$  decoupling with two-pulse phase-modulation (TPPM) [22] can be applied throughout. At the end of the

\* Corresponding author. Fax: +41 21 6939435.

E-mail address: [Simone.Cavadini@epfl.ch](mailto:Simone.Cavadini@epfl.ch) (S. Cavadini).

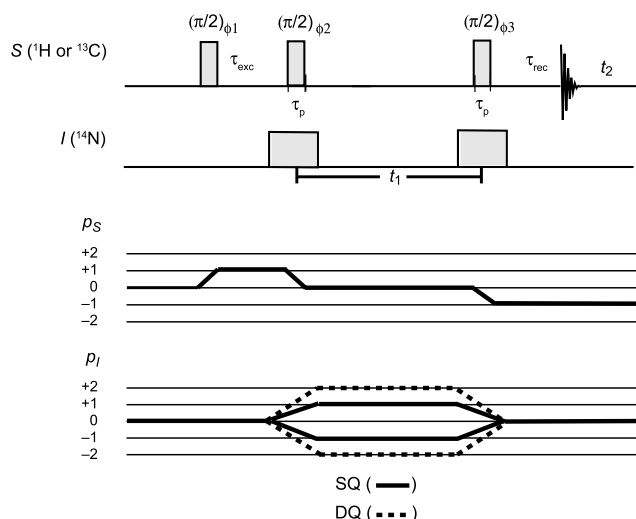


Fig. 1. Pulse sequences for the indirect observation of  $I$  ( $^{14}\text{N}$ ) single-quantum (SQ) or double-quantum (DQ) spectra in solids rotating at the magic angle via spy nuclei  $S$  ( $^1\text{H}$  or  $^{13}\text{C}$ ) by heteronuclear single-quantum correlation (HSQC). The experiment makes use of scalar couplings and second-order quadrupole–dipole cross-terms between  $I$  and  $S$  nuclei during the excitation and reconversion intervals  $\tau_{\text{exc}}$  and  $\tau_{\text{rec}}$  for the transfer of coherence. The coherence transfer pathways for the two spins  $I$  and  $S$  show continuous and dashed lines for SQ and DQ  $^{14}\text{N}$  coherences. When carbons are used as spy nuclei, cross polarization from protons to carbons replaces the first  $(\pi/2)_{\phi_1}^S$  pulse.

excitation interval  $\tau_{\text{exc}}$ , the density operator may comprise a superposition of antiphase terms  $S_\alpha I_z$  and  $S_\alpha I_z^2$  (with  $\alpha = x$  or  $y$ ), bearing in mind that even under fast spinning the spectrum of the spy nucleus  $S$  coupled to  $I = 1$  features inhomogeneous powder patterns, as shown in Fig. 1 of Ref. [10]. If we start with  $S_x$  at the beginning of  $\tau_{\text{exc}}$ , a mixture of  $S_y I_z$  and  $S_x I_z^2$  may result from heteronuclear  $J$  couplings [23,24], while simulations show that only  $S_x I_z^2$  and  $S_y I_z^2$  can arise if we have pure RDS between  $S = 1/2$  and  $I = 1$ . In order to convert  $(S_x I_z \cos \theta + S_y I_z \sin \theta)$  for an arbitrary phase  $\theta$ , into  $S_z I_z$ , and  $(S_x I_z^2 \cos \theta + S_y I_z^2 \sin \theta)$  into  $S_z I_z^2$ , a  $(\pi/2)_{\phi_2}^S$  pulse must be applied to the  $S$  spins with a phase  $\phi_2$  that must be orthogonal to the phase  $\theta$ . This phase depends on the offset  $\Omega^S$  and on the RDS which varies with the orientation of the crystallites. The phase  $\phi_1$  is stepped through  $x, y, -x, -y$ , the phase  $\phi_2$  is alternated between  $4(x)$  and  $4(-x)$  and the phase  $\phi_3$  is not changed, while the receiver phase  $\phi_{\text{rec}}$  is stepped through  $x, -y, -x, y, -x, y, x, -y$ , entailing a two-fold loss of the signal-to-noise ratio compared to HMQC for the same number of scans, as verified experimentally. The signals thus obtained are largely independent of the offset  $\Omega^S$  of the radio-frequency (RF) carrier. Unlike the situation that prevails in liquid-state HSQC, offsets cannot be refocused by applying  $(\pi)^S$  and  $(\pi)^I$  pulses in the middle of the  $\tau_{\text{exc}}$  and  $\tau_{\text{rec}}$  intervals. Magic angle spinning combined with rotor synchronization of the  $\tau_p$  pulses applied to the  $I$  spins averages out the first order quadrupolar interaction. The distinction between SQ and DQ of spin  $I$  can be made as usual with two-step or four-step cycles of one of the  $\tau_p$  pulses applied to the  $I$  spins [10]. The evolution period  $t_1$  is defined as the interval

between the centers of the two  $\tau_p$  pulses. In principle, the insertion of a  $(\pi)^S$  pulse in the middle of  $t_1$  period should lead to line-narrowing in  $\omega_1$  like in liquids, because of the refocusing of both RDS and  $J$  couplings, but in carbon-13 or proton-detected HSQC it was found that the lineshapes were not significantly affected when a  $(\pi)^S$  pulse was inserted. The conversion of  $(S_x I_z \cos \theta + S_y I_z \sin \theta)$  into  $S_z I_z$ , and of  $(S_x I_z^2 \cos \theta + S_y I_z^2 \sin \theta)$  into  $S_z I_z^2$ , makes the lineshape in the  $\omega_1$  domain immune to both homogeneous and inhomogeneous decay of transverse  $S_x$  and  $S_y$  terms in the  $t_1$  interval. Even if the decay of the  $S$ -spin coherences during  $t_1$  (we observed a  $^{13}\text{C}^\alpha$  linewidth of 70 Hz in L-alanine and a  $^1\text{H}^N$  linewidth of 700 Hz in glycine- $d_2$ ) is minor compared to the decay of the  $^{14}\text{N}$  coherences (SQ linewidth 1100 Hz for L-alanine and 1600 Hz for glycine- $d_2$ ; DQ linewidth 2200 Hz for L-alanine and 3200 Hz for glycine- $d_2$ ) in HSQC the resulting second-order quadrupolar  $^{14}\text{N}$  powder patterns appear less distorted in HSQC, allowing the extraction of more accurate quadrupolar parameters by comparison with simulations than in HMQC. This is particularly important when protons are used as spy nuclei. For dilute spins such as carbon-13, the slow dissipation of the longitudinal  $S_z(C_z)$  term in the  $t_1$  evolution period does not significantly affect either  $S_z I_y$  or  $S_z I_y^2$ . Even with proton detection in partly deuterated materials, the dissipation of the  $S_z(H_z)$  operator does not appear to influence the  $S_z I_y$  or  $S_z I_y^2$  terms.

Fig. 2 shows a comparison of  $^{13}\text{C}$ -detected  $^{14}\text{N}$  SQ and DQ spectra recorded with both HSQC and HMQC [10] methods under the same conditions. The signals correspond to the  $^{14}\text{N}^1\text{H}_3^+$  ammonium group in L-alanine that is isotopically enriched in the  $^{13}\text{C}^\alpha$  position. Overall the SQ spectra have roughly half the width of DQ spectra.

The proton-detected HSQC and HMQC  $^{14}\text{N}$  SQ and DQ spectra [9] of the  $^{14}\text{N}^1\text{H}_3^+$  ammonium group in glycine- $d_2$  are shown in Fig. 3. Note that the HSQC spectra feature well-resolved singularities that are partly hidden in the HMQC spectra. These allow one to determine the quadrupolar parameters with enhanced accuracy.

The efficiency of the HSQC method can be estimated from the ratio

$$r_{\text{SQ/DQ}} = \frac{S_{\text{SQ/DQ}}(\tau_{\text{exc}}, t_1 = \tau, \tau_{\text{rec}}, \omega_2)}{S(\tau_{\text{exc}} - (\pi/2)^S - \tau - (\pi/2)^S - \tau_{\text{rec}}, \omega_2)} \quad (1)$$

with  $\tau = 1/\nu_{\text{rot}} - \tau_{(\pi/2)}^S$ . This ratio, which may loosely be regarded as a quantum yield, compares the signal amplitude of the first row  $S_{\text{SQ/DQ}}(\tau_{\text{exc}}, t_1 = \tau, \tau_{\text{rec}}, \omega_2)$  of the 2D spectrum (using phase-cycles appropriate for either  $^{14}\text{N}$  SQ or DQ detection) and the signal amplitude  $S(\tau_{\text{exc}} - (\pi/2)^S - \tau - (\pi/2)^S - \tau_{\text{rec}}, \omega_2)$  of a 1D spectrum obtained by Fourier transformation of an  $S$ -spin signal recorded without any  $^{14}\text{N}$  pulses. The experimental yields of the two-way coherence transfer process in the HSQC experiment of Fig. 1 were found to be  $r_{\text{SQ/DQ}} = 14$  and 10% for  $^{13}\text{C}$ -detected SQ and DQ spectra, respectively. Similar spectra recorded under the same conditions but using the

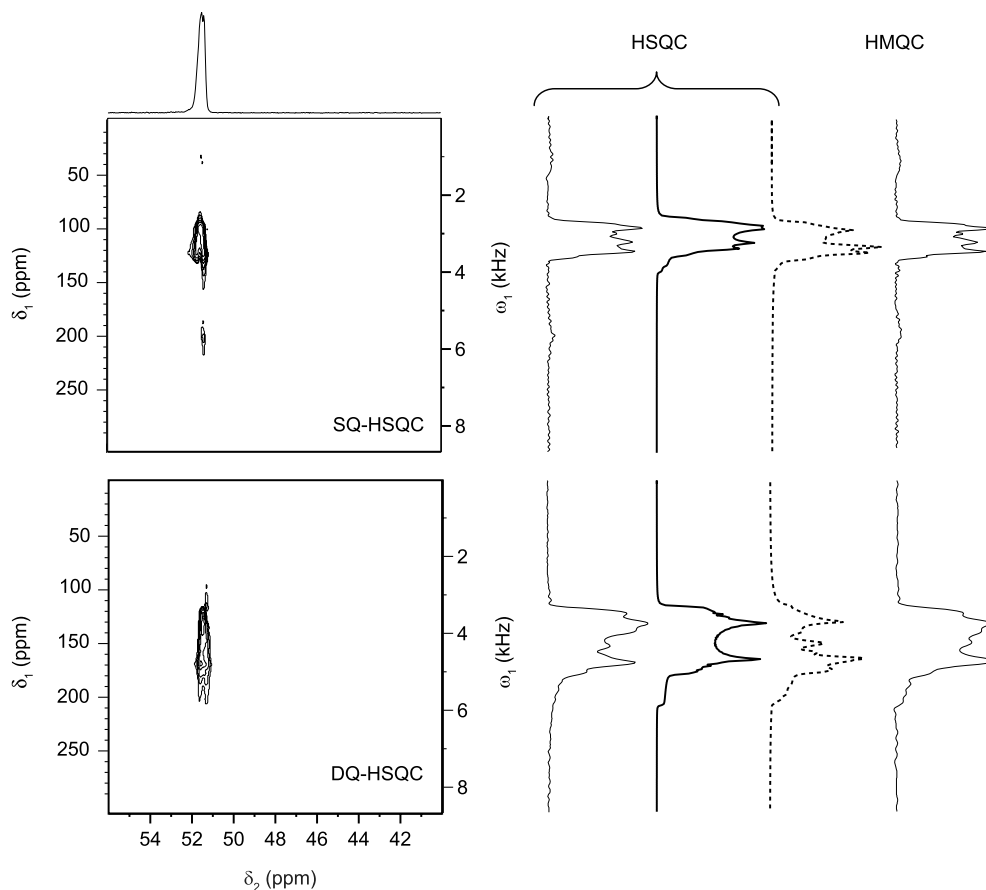


Fig. 2. Experimental two-dimensional carbon-13-detected HSQC spectra showing the  $^{14}\text{N}$  single-quantum (SQ) and double-quantum (DQ) responses of the  $^{14}\text{N}^1\text{H}_3^+$  ammonium group of L-alanine  $\text{NH}_3^+ \text{C}^\alpha \text{HCH}_3\text{COO}^-$  enriched in the  $\text{C}^\alpha$  position. A sample of 11  $\mu\text{l}$  was spun in a 2.5 mm rotor at 30.03 kHz in a static field of 9.4 T (28.9 and 100.6 MHz for  $^{14}\text{N}$  and  $^{13}\text{C}$ ). The fixed delays were set to a compromise  $\tau_{\text{exc}} = \tau_{\text{rec}} = 16$  ms while the  $^{14}\text{N}$  pulse lengths were  $\tau_p = 10$  and 20  $\mu\text{s}$  for SQ and DQ, respectively. The residual dipolar splittings may be seen in the horizontal  $\omega_2$  dimension. The projections onto the vertical  $\omega_1$  axes (thin curves) may be compared with simulations (thick curves) for a hypothetical uniform excitation of all crystallites (4180 orientations) and simulations (dashed curves) taking into account the full HSQC sequence. The quadrupolar parameters in the simulations were  $C_Q = 1.13$  MHz and  $\eta_Q = 0.28$ . For comparison, the projections of two-dimensional HMQC spectra recorded under identical conditions are shown by thin lines on the far right. (Similar spectra were shown elsewhere [10] for  $\tau_{\text{exc}} = \tau_{\text{rec}} = 19$  and 21 ms for SQ and DQ, respectively.) The two-dimensional spectra result from averaging 32 (SQ-HSQC) and 128 (DQ-HSQC) transients for each of 256  $t_1$  increments with  $\Delta t_1 = 1/\nu_{\text{rot}} = 33.3$   $\mu\text{s}$ , and a relaxation interval of 2 s. The spectra were acquired with a carbon carrier at 45 ppm.

$^{13}\text{C}$ -detected HMQC method for the same sample yielded  $r_{\text{SQ/DQ}} = 16$  and 12%, considering an appropriate reference experiment [10]. For proton-detected HSQC the efficiencies were found to be  $r_{\text{SQ/DQ}} = 5.3$  and 1% for SQ and DQ spectra. Under the same experimental conditions, the proton-detected  $^{14}\text{N}$  HMQC experiments had yields of 6 and 1% for SQ and DQ spectra. Antonijevic and Halpern-Manners have reported similar experiments with proton detection but did not dwell on their efficiency [25]. The comparison of experiments and simulations of both SQ and DQ spectra allows one to estimate the quadrupolar parameters for L-alanine  $C_Q = 1.13$  MHz and  $\eta_Q = 0.28$ . For glycine- $d_2$  the quadrupolar parameters were  $C_Q = 1.18$  MHz and  $\eta_Q = 0.5$ .

Deuterated glycine- $d_2$  and L-alanine were purchased from Cambridge Isotope Laboratories and used without further purification. Experimental results were obtained at 9.4 T (28.9, 100.6, and 400 MHz for  $^{14}\text{N}$ ,  $^{13}\text{C}$ , and  $^1\text{H}$ ) with samples packed in 2.5 mm outer diameter  $\text{ZrO}_2$  ro-

tors. The rotors were spun at 30.03 kHz in a Bruker triple-resonance CPMAS probe. With a 1 kW amplifier, the  $^{14}\text{N}$  pulses had an amplitude  $\nu_{\text{RF}} = 57$  kHz, calibrated by direct detection of  $\text{NH}_4\text{NO}_3$ . In the intervals  $\tau_{\text{exc}}$ ,  $t_1$ , and  $\tau_{\text{rec}}$  in Fig. 1, TPPM proton decoupling was used in  $^{13}\text{C}$ -detected experiments with  $\nu_{\text{RF}} = 100$  kHz, pulse-widths of 3.7  $\mu\text{s}$ , and a phase difference between two successive pulses of  $25^\circ$ . During the  $^{13}\text{C}$  acquisition period  $t_2$  a lower  $^1\text{H}$  RF amplitude of  $\nu_{\text{RF}} = 70$  kHz was used, with pulse-widths of 5.2  $\mu\text{s}$  and a phase difference of  $35^\circ$ . The magic angle was adjusted within  $0.01^\circ$  using deuterated  $[\text{D}_6]\alpha$ -oxalic acid dehydrate [26]. The chemical shifts for  $^1\text{H}$ ,  $^{13}\text{C}$ , and  $^{14}\text{N}$  were referred to the external standards of TMS, adamantane, and  $\text{NH}_4\text{Cl}$ , respectively.

**Conclusions.** It has been shown that indirect detection of  $^{14}\text{N}$  spectra via spin  $S = 1/2$  such as  $^1\text{H}$  or  $^{13}\text{C}$  may benefit from using a pulse sequence where the  $S$  spin magnetization is made to be longitudinal in the evolution interval  $t_1$  in the manner of heteronuclear single-quantum correlation

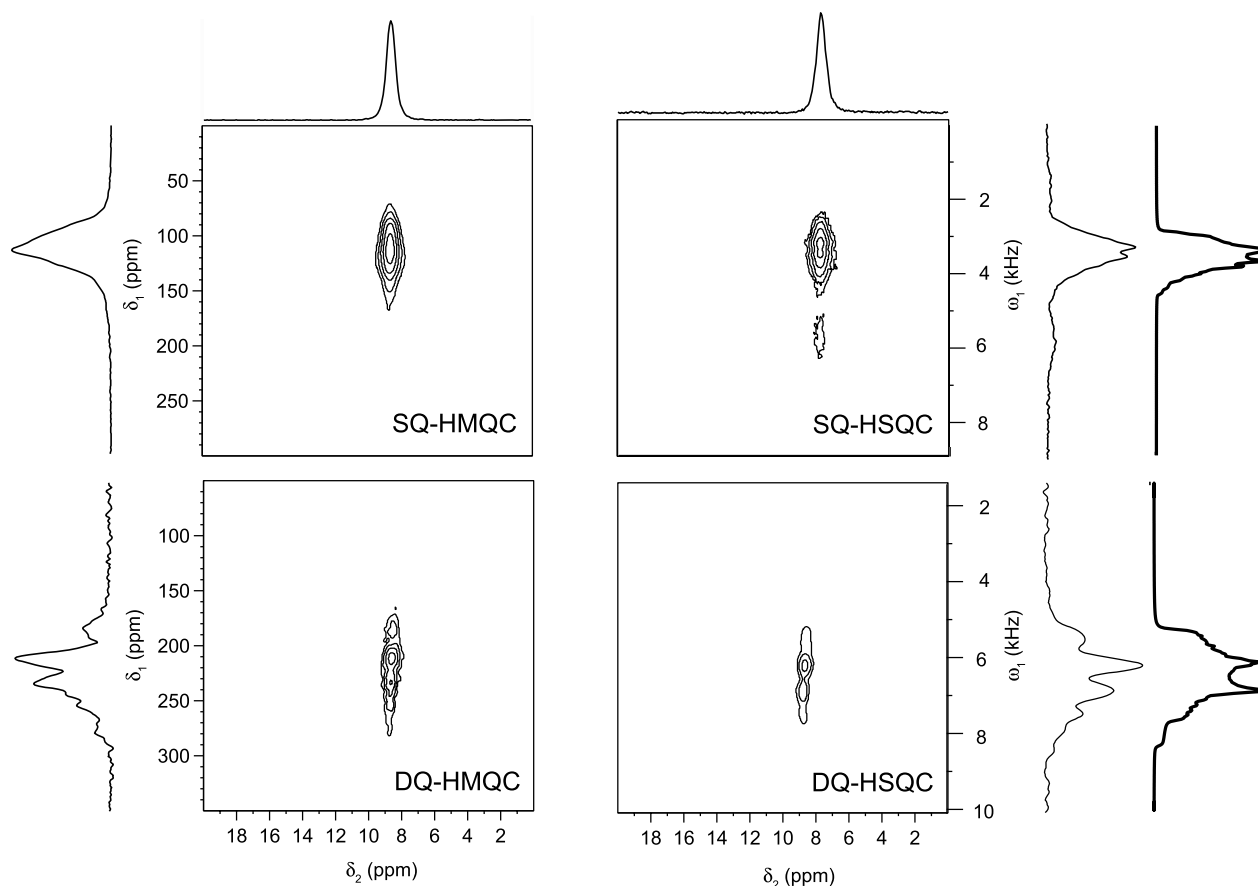


Fig. 3. Proton-detected experimental HMQC and HSQC spectra showing  $^{14}\text{N}$  SQ and DQ signals of the  $^{14}\text{N}^1\text{H}_3^+$  ammonium group in zwitterionic glycine- $d_2$   $\text{NH}_3^+\text{CD}_2\text{COO}^-$  without  $^{13}\text{C}$  enrichment. A sample of 11  $\mu\text{l}$  was spun in a 2.5 mm rotor at 30.03 kHz in a static field of 9.4 T (28.9 and 400 MHz for  $^{14}\text{N}$  and  $^1\text{H}$ ). For the SQ spectra, the  $^{14}\text{N}$  pulse lengths were  $\tau_p = 12 \mu\text{s}$  and  $\tau_{\text{exc}} = \tau_{\text{rec}} = 1 \text{ ms}$ . For the DQ spectra,  $\tau_p = 35 \mu\text{s}$  and  $\tau_{\text{exc}} = \tau_{\text{rec}} = 0.9 \text{ ms}$ . The projections onto the vertical  $\omega_1$  axes (thin curves) may be compared with simulations (bold curves on right-hand side) obtained for a hypothetical uniform excitation of all crystallites (4180 orientations) and rotor synchronization with quadrupolar parameters  $C_Q = 1.18 \text{ MHz}$  and  $\eta_Q = 0.5$ . The two-dimensional spectra result from averaging 128 (SQ) and 256 (DQ) transients for each of 256  $t_1$  increments with  $\Delta t_1 = 1/\nu_{\text{rot}} = 33.3 \mu\text{s}$ , and a relaxation interval of 2 s. The spectra were acquired with a proton carrier at 5 ppm.

(HSQC). This allows one to obtain clean second-order  $^{14}\text{N}$  single- and double-quantum powder patterns that are not distorted by homogeneous or inhomogeneous decay of the coherence of the  $^1\text{H}$  or  $^{13}\text{C}$  spy nuclei in the evolution interval, in contrast to earlier methods that were built on the principle of heteronuclear multiple-quantum correlation (HMQC), where the  $^1\text{H}$  or  $^{13}\text{C}$  spins participate in a coherent superposition of states with the  $^{14}\text{N}$  spins. For carbon detection, we do not observe any significant changes in the  $^{14}\text{N}$  lineshapes using the new HSQC scheme. On the other hand, when protons are used as spy nuclei, the HSQC scheme leads to a gain in resolution.

#### Acknowledgments

We are indebted to Sasa Antonijevic and Nicholas Halpern-Manners for providing a preprint of their work. We acknowledge support of the Fonds National de la Recherche Scientifique (FNRS, Switzerland), of the Commission pour la Technologie et l'Innovation (CTI, Switzerland), and of the Lawrence Berkeley National Laboratory.

#### References

- [1] W.G. Proctor, F.C. Yu, The dependence of a nuclear magnetic resonance frequency upon chemical compound, *Phys. Rev.* 77 (1950) 717.
- [2] R.E. Stark, R.A. Haberkorn, R.G. Griffin,  $^{14}\text{N}$  NMR determination of NH bond lengths in solids, *J. Chem. Phys.* 68 (1978) 1996–1997.
- [3] R. Tycko, P.L. Stewart, S.J. Opella, Peptide plane orientations determined by fundamental and overtone nitrogen 14 NMR, *J. Am. Chem. Soc.* 108 (1986) 5419–5425.
- [4] H.J. Jakobsen, H. Bildsoe, J. Skibsted, T. Giavani,  $^{14}\text{N}$  MAS NMR spectroscopy: the nitrate ion, *J. Am. Chem. Soc.* 123 (2001) 5098–5099.
- [5] R.K. Harris, A.C. Olivieri, Quadrupolar effects transferred to spin-1/2 magic-angle spinning spectra of solids, *Prog. Nucl. Magn. Reson. Spectrosc.* 24 (1992) 435–456.
- [6] J. McManus, R. Kemp-Harper, S. Wimperis, Second-order quadrupolar-dipolar broadening in two-dimensional multiple-quantum MAS NMR, *Chem. Phys. Lett.* 311 (1999) 292–298.
- [7] Z. Gan, Measuring amide nitrogen quadrupolar coupling by high-resolution  $^{14}\text{N}/^{13}\text{C}$  NMR correlation under magic-angle spinning, *J. Am. Chem. Soc.* 128 (2006) 6040–6041.
- [8] S. Cavadini, A. Lupulescu, S. Antonijevic, G. Bodenhausen, Nitrogen-14 NMR spectroscopy using residual dipolar splittings in solids, *J. Am. Chem. Soc.* 128 (2006) 7706–7707.

- [9] S. Cavadini, A. Lupulescu, S. Antonijeivic, G. Bodenhausen, Indirect detection of nitrogen-14 in solids via protons by nuclear magnetic resonance spectroscopy, *J. Magn. Reson.* 182 (2006) 168–172.
- [10] S. Cavadini, A. Lupulescu, S. Antonijeivic, G. Bodenhausen, Indirect detection of nitrogen-14 in solid-state NMR spectroscopy, *ChemPhysChem* 8 (2007) 1363–1374.
- [11] Z. Gan, Rotary resonance echo double resonance for measuring heteronuclear dipolar coupling under MAS, *J. Magn. Reson.* 183 (2006) 235–241.
- [12] Z. Gan,  $^{13}\text{C}/^{14}\text{N}$  heteronuclear multiple-quantum correlation with rotary resonance and REDOR dipolar recoupling, *J. Magn. Reson.* 184 (2006) 39–43.
- [13] Z. Gan, J.P. Amoureux, J. Trébosc, Proton-detected  $^{14}\text{N}$  MAS NMR using homonuclear decoupled rotary resonance, *Chem. Phys. Lett.* 435 (2007) 163–169.
- [14] Z. Gan, D.M. Grant, Rotational resonance in a spin-lock field for solid state NMR, *Chem. Phys. Lett.* 168 (1990) 304–308.
- [15] Z. Gan, D.M. Grant, R.R. Ernst, NMR chemical shift anisotropy measurements by RF driven rotary resonance, *Chem. Phys. Lett.* 254 (1996) 349–357.
- [16] S. Cavadini, A. Abraham, G. Bodenhausen, Proton-detected nitrogen-14 NMR by recoupling of heteronuclear dipolar interactions using symmetry-based sequences, *Chem. Phys. Lett.* 445 (2007) 1–5.
- [17] L. Müller, Sensitivity enhanced detection of weak nuclei using heteronuclear multiple quantum coherence, *J. Am. Chem. Soc.* 101 (1979) 4481–4484.
- [18] D. Massiot, F. Fayon, B. Alonso, J. Trébosc, J.-P. Amoureux, Chemical bonding differences evidenced from  $J$ -coupling in solid state NMR experiments involving quadrupolar nuclei, *J. Magn. Reson.* 164 (2003) 160–164.
- [19] D. Iuga, C. Morais, Z. Gan, D.R. Neuville, L. Cormier, D. Massiot, NMR heteronuclear correlation between quadrupolar nuclei in solids, *J. Am. Chem. Soc.* 127 (2005) 11540–11541.
- [20] A.A. Maudsley, R.R. Ernst, Indirect detection of magnetic resonance by heteronuclear two-dimensional spectroscopy, *Chem. Phys. Lett.* 50 (1977) 368–372.
- [21] G. Bodenhausen, D.J. Ruben, Natural abundance nitrogen-15 NMR by enhanced heteronuclear spectroscopy, *Chem. Phys. Lett.* 69 (1980) 185–189.
- [22] A.E. Bennett, C.M. Rienstra, M. Auger, K.V. Lakshmi, R.G. Griffin, Heteronuclear decoupling in rotating solids, *J. Chem. Phys.* 103 (1995) 6951–6958.
- [23] N. Chandrakumar, Polarization transfer between spin-1 and spin-1/2 nuclei, *J. Magn. Reson.* 16 (1984) 28–36.
- [24] O.W. Sørensen, G.W. Eich, M.H. Levitt, G. Bodenhausen, R.R. Ernst, Product operator formalism for the description of NMR pulse experiments, *Prog. Nucl. Magn. Reson. Spectrosc.* 16 (1983) 163–192.
- [25] S. Antonijeivic, N. Halpern-Manners, Probing amide bond nitrogens in solids using  $^{14}\text{N}$  NMR spectroscopy, private communication.
- [26] S. Antonijeivic, G. Bodenhausen, High-resolution NMR spectroscopy in solids by truly magic-angle spinning, *Angew. Chem.* 117 (2005) 2995–2998; *Angew. Chem. Int. Ed.* 44 (2005) 2935–2938.